The Effects of Tropical Weather on Radio-Wave Propagation Over Foliage Channel

Yu Song Meng, *Student Member, IEEE*, Yee Hui Lee, *Member, IEEE*, and Boon Chong Ng, *Senior Member, IEEE*

***Abstract*—This paper investigates the dynamic property of a tropical forested channel due to the weather effect on very high frequency (VHF) and ultrahigh frequency (UHF) radio-wave propagation. In this paper, continuous-wave (CW) envelope fading waveforms are recorded over a period of 50 s with static antennas. This paper focuses on the analysis of the combined effect of wind and rain, which is often encountered in a tropical forest. The induced temporal effects are discussed and compared with theoretical models. It is found that the distribution of temporal fading components resembles a Rician distribution function. Its Rician K factor gradually decreases as the strength of either wind or rain increases due to the movement of the forest components.**

***Index Terms*—Forest, propagation, ultrahigh frequency (UHF) and weather, very high frequency (VHF).**

I. Introduction

VEGETATION plays a significant role in the fading phenomena in wireless communications [1]–[13]. Much effort has been put into path loss modeling [1]–[5] at various frequencies (very high frequency (VHF) to millimeter band), both theoretically and experimentally, since the 1960s. Different influences on the path loss in a foliage channel, such as types of trees, geometries of the path, height of the antenna, etc., have been discussed. In particular, interest has arisen in the study of weather-induced effects on radio-wave propagation through vegetation [6]–[9]. The seasonal variation of humidity is studied in [6], and the wind-induced temporal variation is examined in [7]–[9]. In [7] and [9], the wind-induced temporal variation on a foliage-obstructed cellular base-to-mobile channel is characterized, modeled, and found to be Rician distributed.

In recent years, there has been a growing interest in the near-ground (0.5–3 m above ground) communication channel within foliage areas at the VHF and UHF bands. Its application is of scientific and military importance [10]–[13]. These applications require a detailed understanding of the forested propagation channel to establish a good communication link. As a supplement to the well-studied path loss models within the foliage channels [1], [3], [10]–[13], the weather-induced effect on the near-ground forested channel needs to be investigated. From the open literature, there is minimal research work done on the weather-induced effect on the foliage channel for near-ground communications, except for the study on wind effects, as reported in [7]–[9] for cellular base-to-mobile channels. In Singapore, tropical weather conditions such as rain and wind are often encountered together. The combined effects of wind and rain cause significant variation to the propagation channel. This variation in propagation channel can affect the reliability of modern communication systems when implemented for use within a forest environment. Therefore, in this paper, the focus is on the characterization and modeling of tropical weather effects on the near-ground forested propagation path.

As a continuation of our previous papers [14], [15], the main objective of this paper is to perform a detailed statistical characterization and modeling of the combined effects of several typical weather phenomena often experienced in the tropical region. The combined effect of wind and rain on a tropical forested channel over the VHF (240 MHz) and UHF (700 MHz) bands for near-ground communications (2.15 m) is studied. The tropical forest under investigation is described in Section II, together with a brief description of the experimental setup. In Section III, a detailed statistical study is performed for the weather effects on the forested radio-wave propagation. This is done by examining the additional attenuation and temporal variations induced by the varying weather conditions. The propagation channel under severe weather conditions of heavy rain and strong wind is analyzed in Section IV. Section V gives a summary of this paper.

II. Measurement Campaign

The measurements are performed in Singapore over a period of two weeks in December 2006 during the northeast monsoon season. This is generally the wettest month of the year with an average monthly rainfall of 280 mm. The foliage chosen for this study is a palm plantation over a nearly flat terrain, as shown in Fig. 1. The terrain mainly consists of soil and sand, with some parts covered with grass. The palm trees are approximately 5.6 m in height and nearly equally spaced at a distance of 7 m apart. The average tree trunk diameter at antenna height is around 0.4 m. The foliage depth covered is 400 m.

The measurements were carried out using continuous-wave transmission at 240 and 700 MHz. Discone antennas with a typical gain of 2.4 dBi were used for transmission and reception. Both antennas were kept stationary inside the forested

Manuscript received August 28, 2008; revised February 25, 2009. First published April 21, 2009; current version published October 2, 2009. This work was supported in part by the Defense Science Technology Agency, Singapore. The review of this paper was coordinated by Prof. Z. Yun.

The authors are with the School of Electrical and Electronic Engineering, Nanyang Technological University, Singapore 639798 (e-mail: meng0006@ntu.edu.sg; eyhlee@ntu.edu.sg; ebcng@ntu.edu.sg).

Color versions of one or more of the figures in this paper are available online at http://ieeexplore.ieee.org.

Digital Object Identifier 10.1109/TVT.2009.2021480

Fig. 1. Plantation under measurement.

channel and at a fixed height of 2.15 m with vertical polarization throughout the measurement. At the transmitter, the radio wave from a signal generator passed through a 10-W high-power amplifier before being fed into the transmit antenna.

At the receiver, the discone antenna was connected to a low-noise amplifier with 2.9-dB noise figure and 20-dB gain before passing into a spectrum analyzer. The span of the spectrum analyzer was set to be 2 kHz around its center frequency to minimize the noise bandwidth. Details of the measurement setup can be found in Fig. 2. A total of 5001 peak marker readings at 0.01-s intervals were recorded by a Labview program through a general purpose interface bus connection in order to study the temporal variations due to the effects of wind and rain.

To study the weather effects on the propagating wave, the weather information is derived from the weather radar located by the National Environment Agency (NEA) [16] on the eastern end of the Island of Singapore. The weather radar covers an elevation angle range from 1° to 40°, a maximum range of 240 km, and a scan rate of 12°, producing a full set of volumetric reflectivity and velocity data of the weather information around Singapore every 4 min. According to the NEA classification system, rain is classified by its rain intensities (RI) as slight rain ($RI < 2$ mm/h), moderate rain (2 mm/h $< RI < 10$ mm/h), and heavy rain ($RI > 10$ mm/h), whereas wind is classified by the wind speed (WS) as light wind ($WS < 20$ km/h), windy (20 km/h $< WS < 40$ km/h), and strong wind ($WS > 40$ km/h). Since the experiment is conducted during the northeast monsoon season, the wind comes from the northeasterly direction. During this measurement, slight rainfall ranges from 0.2 to 1.8 mm/h, moderate rainfall ranges from 2.6 to 8.6 mm/h, and heavy rainfall ranges from 12 to 24.2 mm/h, whereas light wind ranges from 0.7 to 17.6 km/h, windy ranges from 24.1 to 30.7 km/h, and strong wind ranges from 40.6 to 54.1 km/h.

III. Results and Discussions

The typical (representative of more than 78% of all the estimated results) envelope fading waveforms corresponding to the different weather phenomena at 240 and 700 MHz are shown in Fig. 3. It is found that for both frequencies, in general, there is a lower received power as the wind and rain become stronger. This implies that a stronger wind and rain cause higher signal attenuation. The average received signal varies from -63 to -71 dBm and from -84 to -98 dBm for 240 and 700 MHz, respectively, as the strength of rain and wind increases, as shown in Fig. 3. This 8- and 14-dB variation in signal strength that corresponds to the 240- and 700-MHz signal is purely due to the weather-induced effects. Moreover, the temporal power variations and deep fades are more noticeable as the strength of either wind and/or rain increases. Meaning, the fade variations are largely dependent on the wind and rain effects on this tropical foliage channel. This shows the significance of wind and rain effects on the temporal variation of the propagating signal, even in the VHF and UHF range. Therefore, the wind and rain effects have to be taken into account when determining the fade margin for communication systems used in the tropical forest environment. In the following part, the additional attenuation induced by various weather conditions (normalized to the fair weather condition: no rain and no wind) is discussed in detail. The temporal variation of the tropical forested channel is the focus of the analysis in the latter part of this paper.

A. Additional Attenuation Induced by Varying Weather Conditions

The weather-induced effect on the signal attenuation is shown in Table I, where the additional attenuation induced by the rain and wind is normalized to fair weather for their corresponding frequencies of 240 and 700 MHz. It is found that for both frequencies, the tropical weather induces an additional attenuation on the propagating signal. As the strength of either wind and/or rain increases, the additional attenuation correspondingly increases. In particular, the rain is found to be an important factor that affects the radio-wave propagation within the forest environment. Although it is well known that the rainfall affects propagation only at high frequencies of above 5 GHz [17] in free space, it is found to affect the propagation even at low frequencies of VHF and UHF bands within the forest environment in this paper. The observed additional attenuation with the rain effect is mainly due to the accumulation of rain water on the foliage medium that can potentially become an important source of absorption and attenuation of the propagating wave. Moreover, the results in Table I show that the weather effect on the foliage channel is more pronounced at the higher frequency (700 MHz), as compared with the lower frequency (240 MHz). This is because the wavelength ($\sim$0.43 m) for the 700-MHz signal is much smaller than that (1.25 m) for the 240-MHz signal. The wavelength at 700 MHz is comparable with the dimensions of the physical components within the forest environment. For example, the average tree trunk diameter at antenna height is around 0.4 m. This is about one wavelength at 700 MHz and one third of a wavelength at 240 MHz. Therefore, the tree trunk is a better absorber and attenuator at the higher frequency, as compared with the lower frequency. With the accumulation of rain water, the tree trunk can thereby attenuate the signal strength for a higher frequency to a larger extent, as compared with the lower frequency.

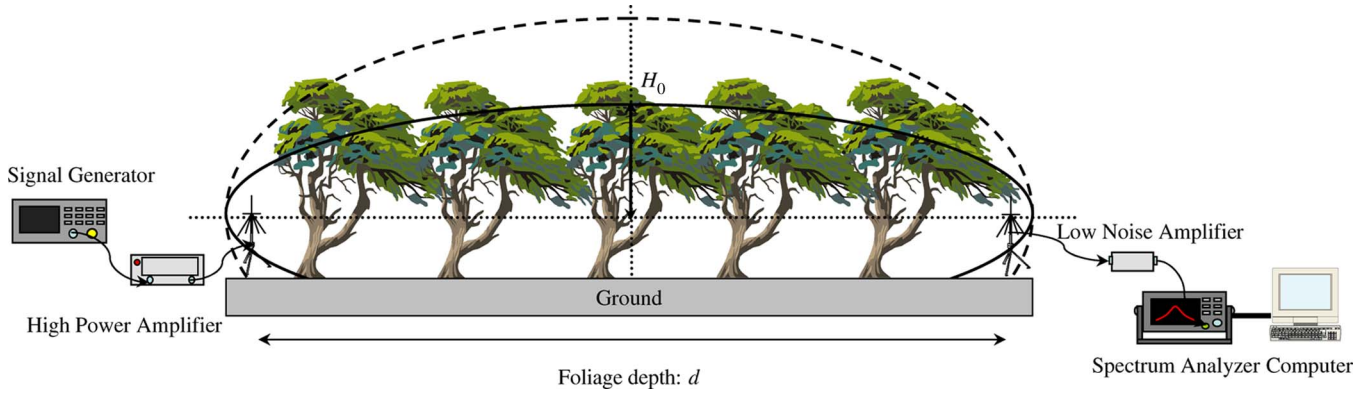

Fig. 2. Schematic diagram of the measurement setup and generic views of the first Fresnel zones (240 MHz _ _ _ _; 700 MHz _____).

B. Weather-Induced Temporal Variations

From Fig. 3, the temporal power variations are observed with the increase in the strength of wind and rain. To model these weather-induced temporal effects, the received signal is normalized to its mean to extract the temporal variations [7], [9]. The temporal variation is usually characterized through the statistical modeling of the signal envelope (amplitude) using the commonly known distributions associated with radio propagation channels [18], namely, Gaussian, Rician, Rayleigh, and Nakagami. The mathematical expressions for each distribution are shown in the following equations.

Gaussian distribution

$$P_r(r) = \frac{1}{\sigma\sqrt{2\pi}} e^{\frac{-(r-\mu)^2}{2\sigma^2}} \tag{1}$$

where μ and σ are the mean and standard deviation of the random variable r.

Rician distribution

$$P_r(r) = \frac{r}{\sigma^2} e^{-\left(\frac{r^2+s^2}{2\sigma^2}\right)} I_0\left(\frac{sr}{\sigma^2}\right) \tag{2}$$

where $I_0(\bullet)$ is the modified Bessel function of the first kind with zeroth order, s is the amplitude of the steady component, and σ^2 is the variance of the random component. In the literature, the Rician distribution function is often described in terms of a fading parameter K, which is commonly known as the Rician K factor, i.e.,

$$K \text{ (in decibels)} = 10\log_{10}\left(\frac{s^2}{2\sigma^2}\right). \tag{3}$$

The physical interpretation of the Rician K factor depends on the type of multipath channel. For a fixed channel where both the transmitter and the receiver are stationary, as in our case, the Rician K factor is the ratio of the mean power to the variance of the received components. This is used to characterize the temporal variability of the propagation channel, which is sensitive to the movements of scattering objects within the propagation channel, such as humans, vehicles, or foliage medium. This Rician K factor varies from $+\infty$ decibels for a static propagation channel with no temporal variations (approaches a Gaussian distribution) to $-\infty$ decibels for a dynamic propagation channel with strong temporal variations (approaches a Rayleigh distribution).

Rayleigh distribution

$$P_r(r) = \frac{r}{\sigma^2} e^{\frac{-r^2}{2\sigma^2}} \tag{4}$$

where σ is the standard deviation of random scattered components.

Finally, Nakagami distribution

$$P_r(r) = \frac{2m^m}{\Gamma(m)\Omega^m} r^{(2m-1)} e^{-\left(\frac{mr^2}{\Omega}\right)} \tag{5}$$

where m and Ω are the shape and scale parameters, respectively, and $\Gamma(\bullet)$ is the gamma function. This is a general fade function that tries to model a combination of distributions. For $m = 1$, this fade distribution reduces to a Rayleigh fade channel, and for $m = (K+1)^2/(2K+1)$, it approximates a Rician fade channel with parameter K, and for $\mathrm{m} = +\infty$, there is no fade in the channel.

The distribution of the measured data is compared with the aforementioned four theoretical distributions. An example of the experimental probability density function (*pdf*) at 700 MHz is plotted in Fig. 4 (with moderate rain and windy conditions). Using the maximum-likelihood estimation (MLE) method in Matlab, the theoretical parameters for the four distributions are estimated [9]. The set of parameters that maximizes the likelihood function to fit the measured data is determined.

To verify how well the distribution of the measured data fits with the theoretical models using the MLE method, the root-mean-square (*RMS*) error E_{rms} between the experimental and theoretical distribution is calculated [4], [9] as follows:

$$E_{\mathrm{rms}} = \sqrt{\frac{\sum_{i=1}^{N}(E_i^2)}{N}} \tag{6}$$

where N is the number of sample points, and E_i is the difference between the experimental and theoretical values at the same fade level. In this test, the average E_{rms} for each distribution under different weather phenomena is calculated and tabulated in Table II. The theoretical model with the smallest E_{rms} is considered to be the best distribution function

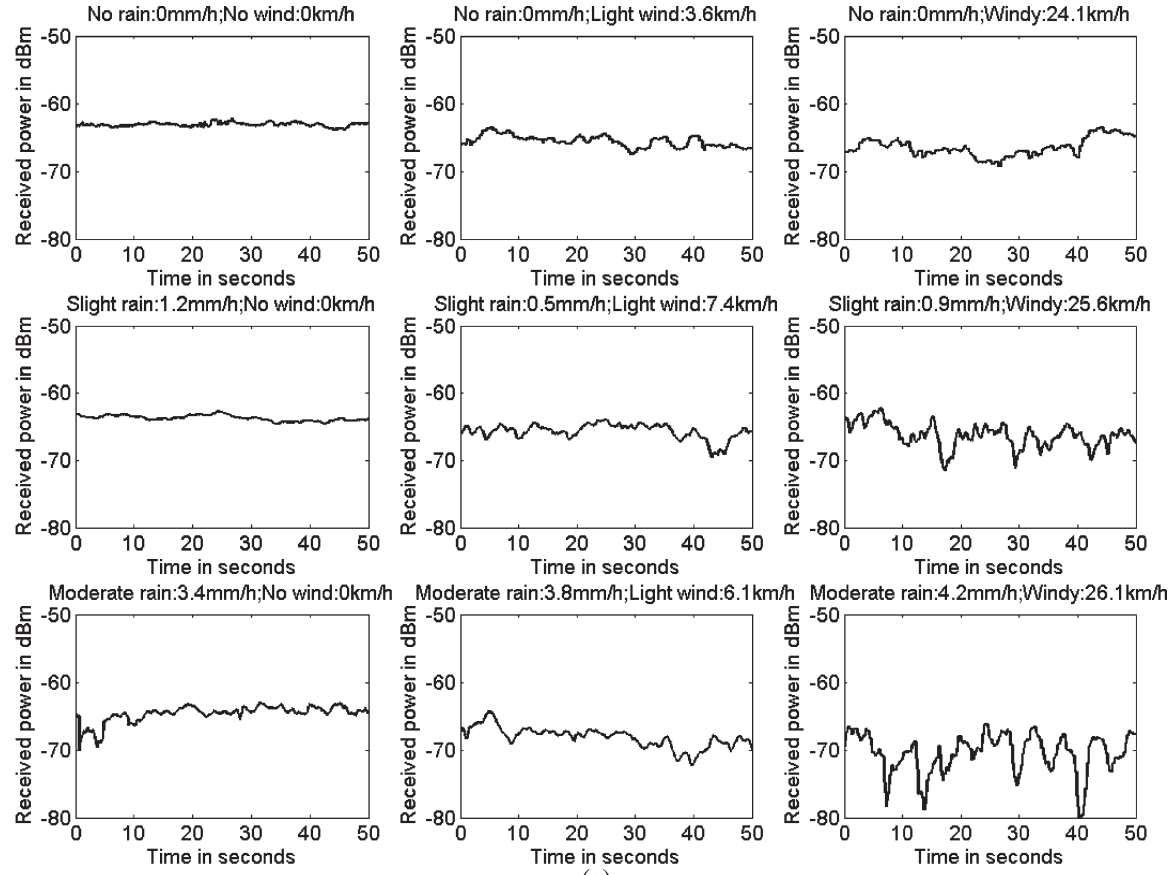

(a)

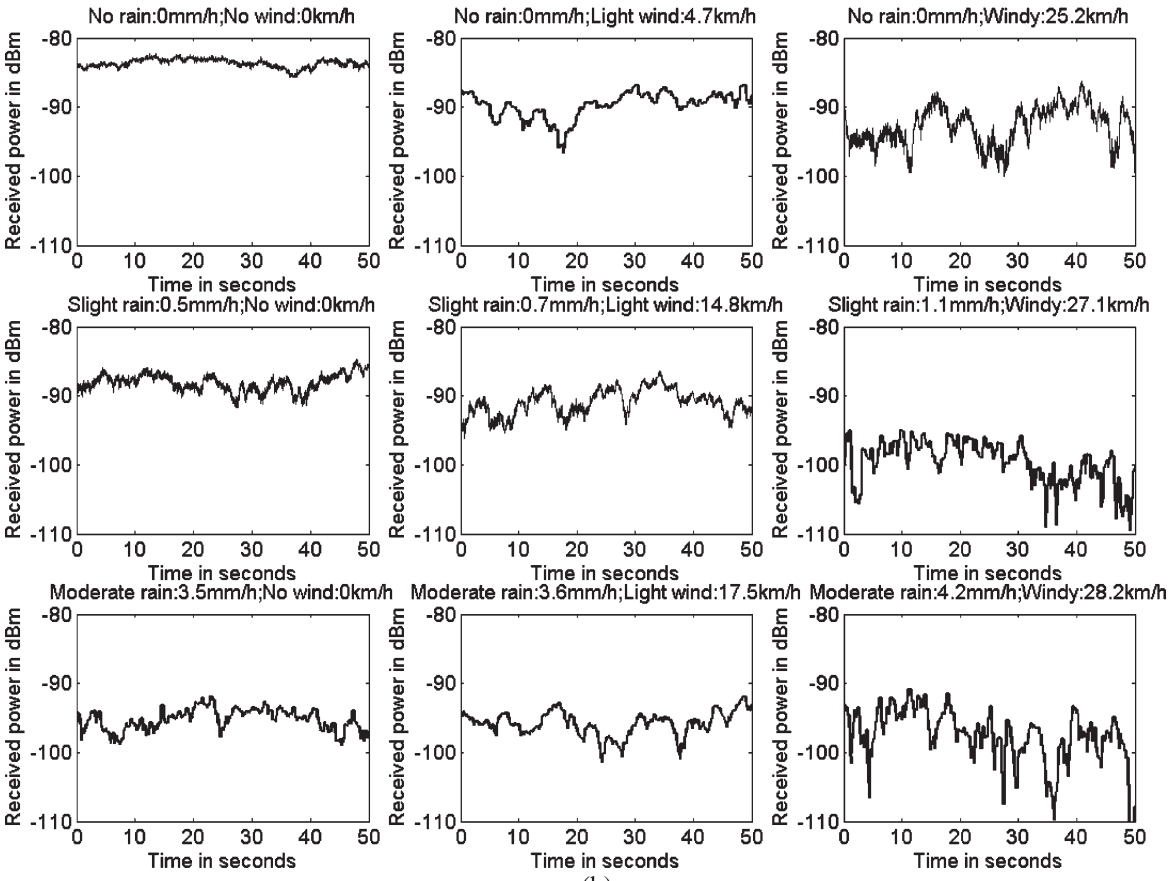

(b)

Fig. 3. Typical received power over time under different weather phenomena. (a) Results at 240 MHz. (b) Results at 700 MHz.

TABLE I
ADDITIONAL ATTENUATION INDUCED BY VARYING WEATHER CONDITIONS ON THE PROPAGATING SIGNAL PER DISTANCE

Frequency	Weather	No wind	Light Wind	Windy
240 MHz	No rain	0 dB/km	6.2 dB/km	8.5 dB/km
	Slight rain	1.5 dB/km	6.5 dB/km	8.1 dB/km
	Moderate rain	3.8 dB/km	12.7 dB/km	18.8 dB/km
700 MHz	No rain	0 dB/km	15.4 dB/km	22.6 dB/km
	Slight rain	11.1 dB/km	18.2 dB/km	40.2 dB/km
	Moderate rain	29.2 dB/km	30.6 dB/km	35.4 dB/km

These results are normalized to the fair weather condition (*i.e.* no rain and no wind).

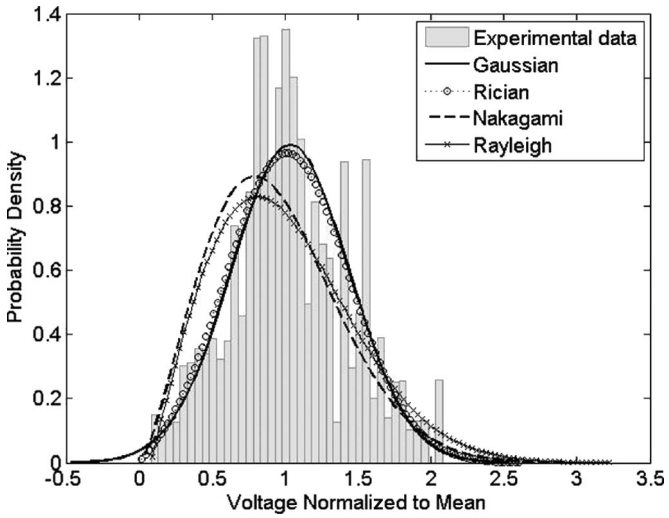

Fig. 4. Example of a *pdf* derived from the measured data fitted with different distribution functions at 700 MHz.

of the four for describing the weather-induced temporal variations of the channel.

From Table II, the Rician and Gaussian distribution functions are found to be the two models with good fit for the description of weather-induced temporal variations for both frequencies (240 and 700 MHz) in general. Since the Rician function is a generally good approximation for the weather-induced temporal variation [7], [9], it will be used for the analysis of the experimental results in this paper. Furthermore, the physical interpretation of its Rician K factor provides an effective and convenient means of performing a comparison of the statistical analysis for different weather and foliage effects. The moment method [19] is then used to determine the Rician K factor of the received signals under different weather conditions. The estimated Rician K factor is tabulated in Table III.

From Table III, it can be seen that, in general, the Rician K factor decreases as the strength of either wind or rain increases for both frequencies. This is due to the movement of the physical elements (leaves and branches) caused by the wind and rain within the foliage channel. The movement increases as the strength of the wind and rain increases, thereby increasing the temporal variability of the propagation channel. However, it is interesting to note that, even without the effects of wind, the falling rain can also decrease the temporal Rician K factor. This is because, in this plantation, the palm trees have broad leaves, as shown in Fig. 1. These broad palm leaves are easily moved by the falling raindrops.

Furthermore, it is also observed that under similar weather conditions, in general, at higher frequency (700 MHz), there is a lower Rician K factor. This is because, at higher frequency, the wavelength is smaller and is thus more comparable with the size of the physical elements in the forested channel. Therefore, higher frequencies (700 MHz) more readily get affected by the variation in weather conditions and thus result in a lower Rician K factor.

IV. FURTHER ANALYSIS ON HEAVY RAIN AND STRONG WIND CONDITIONS

In tropical and equatorial regions, extreme weather conditions with heavy rainfall and strong wind are very often encountered in the form of thunderstorms. This weather condition is very common during the Northeast Monsoon season (when the measurement campaign was conducted). In our measurement campaigns, the data for the extreme weather conditions are limited due to the halt in measurements when there was thunder and lightning. In this section, the limited data collected in heavy rain and strong wind conditions are analyzed. The typical results of heavy rain and strong wind effect on the propagation channel for 240 and 700 MHz, respectively, are shown in Fig. 5. The corresponding additional attenuation induced by this weather condition, which is normalized to fair weather, is found to be 43.7 and 62.2 dB/km for 240 and 700 MHz, respectively. The temporal variation of the received signal is also found to be Rician distributed, and its Rician K factor is -3.19 and -1.99 dB for 240 and 700 MHz, respectively.

Similar to the results presented in the previous section, it can be concluded that either rain or wind can impose an additional attenuation on the propagating wave within the forest environment. The additional attenuation will increase as the strength of the wind and rain increases. Similarly, the additional attenuation increases as the frequency increases. When the propagation channel experiences extreme weather conditions, the additional attenuation can be up to 43.7 and 62.3 dB/km for 240 and 700 MHz, respectively. This can be above the dynamic range of a terrestrial communication link and can cause the breakdown of the link.

The Rician K factor decreases as the strength of the wind and rain increases. This is due to the weather-induced movement of

TABLE II
AVERAGE E_{rms} VALUES FOR EACH DISTRIBUTION UNDER DIFFERENT WEATHER PHENOMENA. (a) AT 240 MHz. (b) AT 700 MHz

(a)

Weather phenomena		Gaussian E_{rms}	Rician E_{rms}	Rayleigh E_{rms}	Nakagami E_{rm}
No rain	No wind	0.0243	0.0243	0.0962	0.0864
	Light Wind	0.0240	0.0240	0.0376	0.1159
	Windy	0.0567	0.0565	0.0458	0.0928
Slight rain	No wind	0.0254	0.0254	0.0262	0.0603
	Light Wind	0.0435	0.0436	0.1312	0.1254
	Windy	0.0261	0.0259	0.0577	0.0755
Moderate rain	No wind	0.0839	0.0840	0.1810	0.1300
	Light Wind	0.0354	0.0355	0.0714	0.0701
	Windy	0.0220	0.0223	0.0650	0.1070

(b)

Weather phenomena		Gaussian E_{rms}	Rician E_{rms}	Rayleigh E_{rms}	Nakagami E_{rm}
No rain	No wind	0.0217	0.0217	0.1116	0.0533
	Light Wind	0.0432	0.0435	0.1114	0.1483
	Windy	0.0339	0.0324	0.0272	0.0249
Slight rain	No wind	0.0111	0.0110	0.0651	0.0269
	Light Wind	0.0216	0.0212	0.0326	0.0172
	Windy	0.0255	0.0255	0.0501	0.0906
Moderate rain	No wind	0.0178	0.0178	0.0343	0.0849
	Light Wind	0.0176	0.0176	0.0764	0.1024
	Windy	0.0248	0.0222	0.0626	0.0415

TABLE III
RICIAN K FACTOR UNDER DIFFERENT WEATHER PHENOMENA

Frequency	Weather	No wind	Light Wind	Windy
240 MHz	No rain	26.51 dB	17.07 dB	12.64 dB
	Slight rain	23.17 dB	15.80 dB	10.19 dB
	Moderate rain	15.72 dB	11.75 dB	7.48 dB
700 MHz	No rain	20.07 dB	11.23 dB	6.31 dB
	Slight rain	13.82 dB	9.86 dB	6.52 dB
	Moderate rain	11.97 dB	10.83 dB	3.43 dB

the foliage medium. The movement increases as the strength of the wind and rain increases, which thereby increases the variation of the received signal strength. However, the same trend for the Rician K factor is not observed as the frequency increases. In the previous section, the Rician K factor is consistently smaller for 700 MHz, as compared with those at 240 MHz. In this section, when the propagation channel experiences heavy rain and strong wind conditions, the Rician K factor at 700 MHz (-1.99 dB) is larger than the Rician K factor at 240 MHz (-3.19 dB).

This can be explained with the help of the first Fresnel zone, since the energy transmission from the transmitter to the receiver is mainly concentrated within this region. The size of the first Fresnel zone surrounding the geometrical ray paths, as shown in Fig. 2, can be computed from the following expression [2]:

$$H_0 = \frac{1}{2}\sqrt{\lambda d} \tag{7}$$

where H_0 is the semiminor axis of the ellipse that forms the outer bound of the first Fresnel zone, λ is the wavelength, and d is the foliage depth covered, as shown in Fig. 2. The estimated H_0 are 11.2 and 6.5 m for 240 and 700 MHz, respectively. Comparing this estimated H_0 of the first Fresnel zone with the

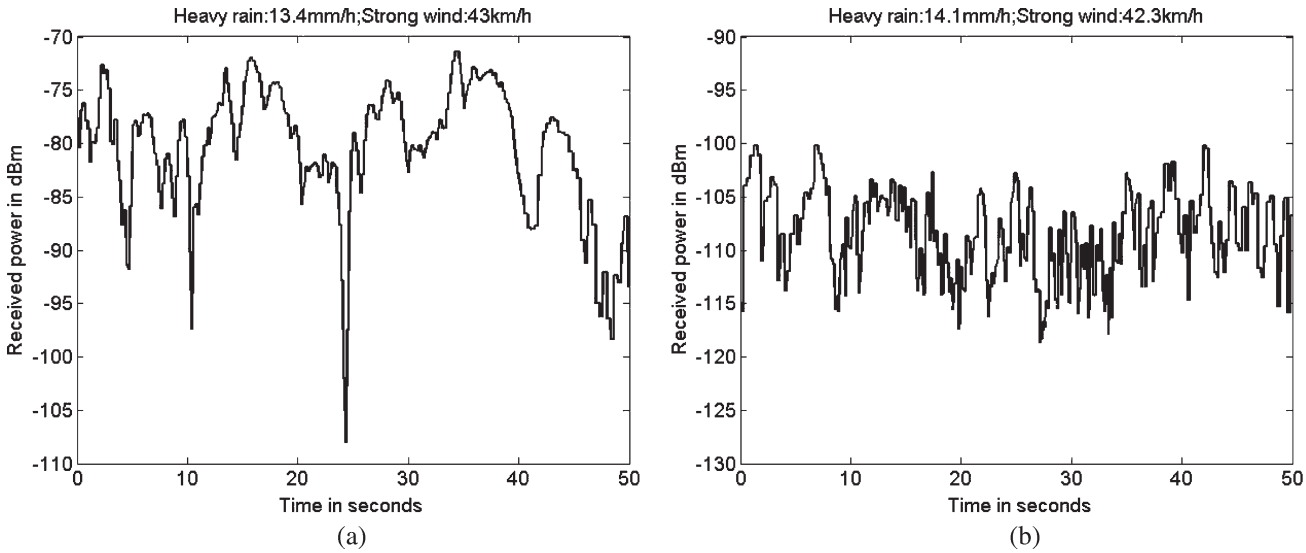

Fig. 5. Typical received power over time during a thunderstorm, where heavy rain and strong wind are experienced. (a) 240 MHz. (b) 700 MHz.

antenna height of 2.15 m and the palm tree canopy height of 5.6 m, it is found that there are relatively little amount of randomly distributed broad leaves of the palm tree that falls within the first Fresnel zone for 700 MHz, as compared with 240 MHz (see Fig. 2). Meaning, most of the first Fresnel zone for 700 MHz is occupied by tree trunks, whose movements due to heavy rain and strong wind are limited as compared with the movement of broad leaves and branches, which have significant contributions within the first Fresnel zones at 240 MHz. This may be the main reason for the lower Rician K factor at 240 MHz, as compared with 700 MHz under the extreme weather condition.

Furthermore, due to the increase in amount of leaves and branches included in the first Fresnel zone at lower frequencies, there is a larger Rician K factor variation of 29–30 dB due to weather variations at 240 MHz, as compared with the Rician K factor variation of 22–23 dB at 700 MHz. This indicates that, at higher frequencies, the relative increase in the temporal variability of the foliage propagation channel is significantly less than those at lower frequencies when the weather conditions change from fair (no rain and no wind) to extreme (heavy rain and strong wind).

V. Conclusion

The effects of natural weather conditions, such as wind and rain, have been examined in this paper. To study the realistic wind and rain effects on a tropical forested channel at VHF and UHF bands, measurements were carried out over a period of two weeks in a palm plantation located on the tropical island of Singapore during the northeast monsoon season, which is the wettest month of the year.

The experimental results indicate that the wind and rain can impose an additional attenuation on the propagation signal within the forest environment. The additional attenuation increases as the strength of the wind and rain increases. This additional attenuation also increases as the frequency increases. It is also observed that there is a large power variation and deep fades in the received signal as the strength of the wind and the intensity of the rain increase.

The temporal fading components due to the weather-induced variation is then statistically modeled and found to be Rician distributed. The decrement of the Rician K factor as the strength of the wind and rain increases indicates an increase in the temporal variability of the propagation channel. In general, the higher frequency signal (700 MHz) has a smaller Rician K factor as compared with the lower frequency signal (240 MHz). This is because the wavelength (0.43 m) for the 700-MHz signal is smaller than that (1.25 m) for the 240-MHz signal. The wavelength of the 700-MHz signal is comparable with the dimensions of the physical elements within the forest; therefore, it is easily affected by the movement of the elements within the forest environment. However, a larger Rician K factor is observed at 700 MHz, as compared with 240 MHz under extreme weather conditions with heavy rain and strong wind. This is because the first Fresnel zone decreases in volume as the frequency increases, thus excluding most of the more moveable scatterers such as leaves and branches. The relatively less variation in the Rician K factor indicates less moveable scatterers within its first Fresnel zone at higher frequency. This paper is useful for the design of a fade margin for a VHF/ UHF communication system in a tropical forested environment.

Acknowledgment

The authors would like to thank the anonymous reviewers and the Associate Editor for their constructive comments and suggestions for this paper.

References

[1] T. Tamir, "On radio-wave propagation in forest environments," *IEEE Trans. Antennas Propag.*, vol. AP-15, no. 6, pp. 806–817, Nov. 1967.
[2] M. L. Meeks, "VHF propagation over hilly, forested terrain," *IEEE Trans. Antennas Propag.*, vol. AP-31, no. 3, pp. 483–489, May 1983.

[3] R. K. Tewari, S. Swarup, and M. N. Roy, "Radio wave propagation through rain forests of India," *IEEE Trans. Antennas Propag.*, vol. 38, no. 4, pp. 433–449, Apr. 1990.
[4] M. O. Al-Nuaimi and A. M. Hammoudeh, "Measurements and predictions of attenuation and scatters of microwave signals by tress," *Proc. Inst. Elect. Eng.—Microw. Antennas Propag.*, vol. 141, no. 2, pp. 70–76, Apr. 1994.
[5] N. C. Rogers, A. Seville, J. Richter, D. Ndzi, N. Savage, R. F. S. Caldeirinha, A. K. Shukla, M. O. Al-Nuaimi, K. Craig, E. Vilar, and J. Austin, "A generic model of 1–60 GHz radio propagation through vegetation," Radiocommun. Agency, London, U.K., May 2002. Final Rep.
[6] K. Low, "UHF measurement of seasonal field-strength variations in forests," *IEEE Trans. Veh. Technol.*, vol. 37, no. 3, pp. 121–124, Aug. 1988.
[7] J. C. R. Dal Bello, G. L. Siqueira, and H. L. Bertoni, "Theoretical analysis and measurement results of vegetation effects on path loss for mobile cellular communication systems," *IEEE Trans. Veh. Technol.*, vol. 49, no. 4, pp. 1285–1293, Jul. 2000.
[8] E. R. Pelet, J. E. Salt, and G. Wells, "Effect of wind on foliage obstructed line-of-sight channel at 2.5 GHz," *IEEE Trans. Broadcast.*, vol. 50, no. 3, pp. 224–232, Sep. 2004.
[9] M. H. Hashim and S. Stavrou, "Measurements and modelling of wind influence on radio wave propagation through vegetation," *IEEE Trans. Wireless Commun.*, vol. 5, no. 5, pp. 1055–1064, May 2006.
[10] L. W. Li, C. K. Lee, T. S. Yeo, and M. S. Leong, "Wave mode and path characteristics in an inhomogeneous anisotropic forest environment," *IEEE Trans. Antennas Propag.*, vol. 52, no. 9, pp. 2445–2455, Sep. 2004.
[11] D. Liao and K. Sarabandi, "Near-earth wave propagation characteristics of electric dipole in presence of vegetation or snow layer," *IEEE Trans. Antennas Propag.*, vol. 53, no. 11, pp. 3747–3756, Nov. 2005.
[12] F. Wang and K. Sarabandi, "A physics-based statistical model for wave propagation through foliage," *IEEE Trans. Antennas Propag.*, vol. 55, no. 3, pp. 958–968, Mar. 2007.
[13] G. G. Joshi, C. B. Dietrich, C. R. Anderson, W. G. Newhall, W. A. Davis, J. Isaacs, and G. Barnett, "Near-ground channel measurements over line-of-sight and forested paths," in *Proc. Inst. Elect. Eng.—Microw. Antennas Propag.*, Dec. 2005, vol. 152, pp. 589–596.
[14] Y. H. Lee and Y. S. Meng, "Tropical weather effects on foliage propagation," in *Proc. 2nd EuCAP*, Edinburgh, U.K., Nov. 2007, pp. 1–5.
[15] Y. S. Meng, Y. H. Lee, and B. C. Ng, "Investigation of rainfall effect on forested radio wave propagation," *IEEE Antennas Wireless Propag. Lett.*, vol. 7, pp. 159–162, 2008.
[16] National Environment Agency. [Online]. Available: http://www.nea.gov.sg/
[17] *Propagation Data and Prediction Methods Required for the Design of Terrestrial Line-of-Sight Systems*, Int. Telecommun. Union, ITU-R P.530-12, Jan. 2007.
[18] T. Rappaport, *Wireless Communications: Principles and Practice*, 2nd ed. Englewood Cliffs, NJ: Prentice–Hall PTR, 2002.
[19] L. J. Greenstein, D. G. Michelson, and V. Erceg, "Moment-method estimation of the Ricean K-factor," *IEEE Commun. Lett.*, vol. 3, no. 6, pp. 175–176, Jun. 1999.

Yu Song Meng (S'09) received the B.Eng. (Hons.) degree in electrical and electronics engineering in 2005 from Nanyang Technological University, Singapore, where he is currently working toward the Ph.D. degree.

Since May 2008, he has been a Research Engineer with the School of Electrical and Electronic Engineering, Nanyang Technological University. His research interest includes wireless channel characterizations and modeling and channel sounder design.

Yee Hui Lee (S'96–M'02) received the B.Eng. (Hons.) and M.Eng. degrees in electrical and electronics engineering from Nanyang Technological University, Singapore, in 1996 and 1998, respectively, and the Ph.D. degree from the University of York, York, U.K., in 2002.

Since July 2002, she has been an Assistant Professor with the School of Electrical and Electronic Engineering, Nanyang Technological University. Her research interests are in antenna design, evolutionary techniques, computational electromagnetics, channel characterization, and rain propagation.

Boon Chong Ng (S'85–M'88–SM'06) received the B.Eng. degree (Hons.) in electrical engineering from the National University of Singapore, Singapore, in 1988 and the M.Sc. degree in electrical engineering, the M.Sc. degree in statistics, and the Ph.D. degree in electrical engineering from Stanford University, Stanford, CA, in 1990, 1996, and 1998, respectively.

From 1988 to 1989 and 1990 to 1993, he was a Research Engineer with the Defense Science Organization (DSO), Singapore. In 1998, he was a Research Assistant with the Information Systems Laboratory, Stanford University. He is currently the Head of the Advanced Communications Laboratories and is a Principal Member of the technical staff with DSO National Laboratories. He is also an Adjunct Associate Professor with the School of Electrical and Electronic Engineering, Nanyang Technological University. He leads research and development groups in multiple-input–mulitiple-output communications, software, and cognitive radios.

Dr. Ng was the recipient of the Singapore Government Defence Technology Training Award (DTTA) Postgraduate Fellowship from 1993 to 1997.